HHS Public Access

Author manuscript

J Am Chem Soc. Author manuscript; available in PMC 2017 October 16.

Published in final edited form as:

J Am Chem Soc. 2017 July 12; 139(27): 9108–9111. doi:10.1021/jacs.7b03044.

Tetranuclear Manganese Models of the OEC Displaying Hydrogen Bonding Interactions: Application to Electrocatalytic Water Oxidation to Hydrogen Peroxide

Zhiji Han, **Kyle T. Horak**, **Heui Beom Lee**, and **Theodor Agapie***

Division of Chemistry and Chemical Engineering, California Institute of Technology, Pasadena, California 91125, United States

Abstract

Toward the development of structural and functional models of the oxygen evolving complex (OEC) of photosystem II (PSII), we report the synthesis of site-differentiated tetranuclear manganese complexes featuring three six-coordinate and one five-coordinate Mn centers. To incorporate biologically relevant second coordination sphere interactions, substituents capable of hydrogen bonding are included as pyrazolates with phenylamino groups. Complexes with terminal anionic ligands, OH^- or Cl^-, bound to the lower coordinate metal center are supported through the hydrogen-bonding network in a fashion reminiscent to the enzymatic active site. The hydroxide complex was found to to be a competent electrocatalyst for O-O bond formation, a key transformation pertinent to the OEC. In an acetonitrile-water mixture, at neutral pH, electrochemical water oxidation to hydrogen peroxide was observed, albeit with low (15%) Faradaic yield, likely due to competing reactions with organics. In agreement, 9,10-dihydroanthracene is electrochemically oxidized in the presence of this cluster both via H-atom abstraction and oxygenation at ~50% combined Faradaic yield.

Graphical abstract

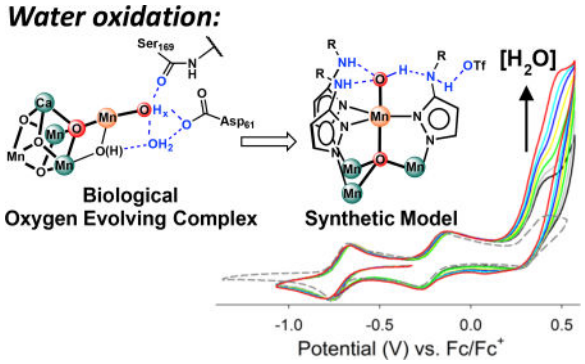

***Corresponding Author**. agapie@caltech.edu.

ASSOCIATED CONTENT

Supporting Information

This material is available free of charge via the Internet at http://pubs.acs.org. Crystallographic data (CIF). General considerations, physical methods, and synthetic procedure. Figures S1–S18, Table S1 (PDF)

The authors declare no competing financial interests.

Water oxidation as source of reducing equivalents for artificial photosynthesis is an appealing approach to solar energy conversion and storage.[1] The oxygen evolving complex (OEC) of photosystem II (PSII) is the biological catalyst for water oxidation to O_2.[2] The OEC features a multinuclear active site, $CaMn_4O_5$, consisting of a cubane $CaMn_3O_4$ moiety connected to a "dangling" Mn center; this cluster coordinates water ligands that are engaged in hydrogen bonding networks (Figure 1A).[2a, 3] Significant efforts have been focused on elucidating the mechanism of water oxidation by the OEC in PSII.[2a, 4] Given the complexity of PSII and the challenge to perform structure-function studies with the biological system, discrete cluster models have been targeted to provide insight into the function of the OEC.[5] Synthetic cluster models that display both Ca and Mn centers and a cubane moiety have been prepared, though they do not display catalytic activity.[6] Multinuclear Mn complexes capable of O-O bond formation are rare.[2b, 2d, 7] More generally, several discrete clusters of first row transition metals with structures reminiscent of the OEC have been reported to support O_2 evolution, although *in situ* formed heterogeneous metal oxides can be responsible for catalysis.[2b, 7g–i, 8] In some cases, the substrate oxygen has been proposed to be a terminal metal-oxo species.[2a,2b] Deprotonations are an integral part of the conversion of water to such moiety. Furthermore, challenging redox steps can be facilitated by coupling of electron and proton transfers.[9] Toward gaining insight into the roles of protons in the chemistry of transition metals with oxygen, a variety of elegant strategies have been reported for supporting transition metal oxo and hydroxo chemistry with hydrogen bonding networks in mononuclear complexes.[10] Such strategies are significantly limited in the context of multinuclear complexes. Moreover, terminal oxo or hydroxo ligands are rare in multinuclear models of the OEC.[11] Herein, we report a synthetic strategy to access a Mn_4 cluster model of the OEC that has a dangling Mn motif, a terminal OH ligand, and second coordination sphere H-bonding to stabilize it (Figure 1B). This species demonstrates O-O bond formation under electrochemical conditions.

Tetranuclear Mn_4 complexes were prepared in a one pot procedure starting from trinuclear precursor $LMn_3(OAc)_3$ **1** (Scheme 1). Addition of $Ca(OTf)_2$ (1.6 equiv) and [RNHPz]Na (3.5 equiv) to **1**,[12] followed by iodosobenzene (PhIO) (1.0 equiv) and Mn(II) salt (1–2 equiv) results in the desired tetramanganese complexes. $Ca(OTf)_2$ facilitates the substitution of acetate ligands with pyrazolates. PhIO acts as the O-atom source for the incorporation of the interstitial oxide moiety. The additional equivalent of Mn(II) is the source of apical metal in the final cluster.[13] Using [PhNHPz]Na as the bidentate ligand and $MnCl_2$ as Mn(II) precursor gave $[LMn_3(PhNHPz)_3OMnCl][OTf]$ (**2**) in ~55% isolated yield. ESI-MS and single crystal X-ray diffraction (XRD, *vide infra*) characterization is consistent with this assignment. A similar synthetic strategy was applied to target a lower coordinate or triflate complex by using $Mn(OTf)_2$ as the fourth equivalent source. ESI-MS characterization of this product suggests the formation of a hydroxide complex. X-ray diffraction quality crystals of this compound have not been obtained to date using the [PhNHPz]Na as the bridging ligand. However, using [4-*t*BuC_6H_4NHPz]Na resulted in a complex with ESI-MS data corresponding to a hydroxide species ($[LMn_3(4\text{-}tBuC_6H_4NHPz)_3OMn(OH)][OTf]$, **3**) that gave crystals suitable for XRD studies.

Solid-state structures of **2** and **3** were determined by XRD (Scheme 1). In both structures, the three basal Mn centers are in a distorted octahedral coordination environment with two bridging alkoxides, one pyrazolate, two pyridine, and a μ_4-oxo ligands each. The apical Mn displays a trigonal bipyramidal geometry and is connected to the three basal Mn centers through the interstitial μ_4-oxo ion. The Cl(1)-N(1) distance (3.056(7) Å) in **2** is slightly shorter than the range (3.238–3.326 Å) observed in a previously reported five coordinate mononuclear Mn-Cl complex with intramolecular hydrogen bonding networks indicating that all NH bonds engage in dative hydrogen bonding interactions with the chloride.[14]

The Mn-μ_4-oxo distances in **3** are consistent with the presence of two Mn(II) (Mn(3) and Mn(4)) and two Mn(III) (Mn(1) and Mn(2)).[13] These oxidation state assignments, charge balance, and localization of OH and NH hydrogens in the electron density map support the assignment of the apical ligand as a hydroxide. Compound **3** displays two short O-N distances between the hydroxide oxygen and the aniline nitrogens (2.774(5) and 2.805(7) Å, for N(1) and N(2), respectively). These distances correspond to strong hydrogen bonding interactions, in the range previously reported (2.721–2.848 Å) for mononuclear Mn(III)-oxo species.[10a] The geometry at nitrogen is consistent with the two anilines acting as hydrogen bond donors to the hydroxide lone pairs. The third O-N distance is longer (2.939(5) Å, to N(3)), and the orientation is consistent with the aniline serving as the hydrogen bond acceptor. The N(3)H bond acts as a hydrogen bond donor to a triflate ion. The differences in the hydrogen bonding interactions in **2** vs **3** highlight the versatility of the aniline moiety in accommodating both donor and acceptor functions. The Mn(1)-O(2) distance (1.874(3) Å) is comparable to a mononuclear complex displaying an intramolecular hydrogen bonding network, at 1.872(2) Å, suggesting that the coordination environment for the Mn(1)-OH moiety is similar to monomanganese species despite being part of a cluster.[10a] All structural parameters are consistent with a cluster supporting a Mn(III)-coordinate terminal hydroxide that is engaged in several hydrogen bonds. Although the geometry of the donors and acceptors differs, the structural parameters are similar between the OEC and **3**; the three non-hydrogen atoms closest to one of the OEC terminal oxygenic ligand are in the range of 2.67–3.04 Å (Figure 1),[3d] which includes the range observed in 3 for the O(2)-N distances.

The electrochemical properties of **3** were investigated by cyclic voltammetry (Figure 2). Two reversible one-electron redox events are observed at −0.72 and −0.21 and a quasireversible redox couple at 0.35 V vs Fc/Fc^+. In the context of water oxidation by the OEC, the electrochemical behavior of **3** in the presence of water is of interest. Independently, compound **3** was found to be soluble and stable in $MeCN/H_2O$ mixtures containing up to 10 % volume water as observed by ^1H NMR spectroscopy (Figure S13). The CV of **3** was recorded in the presence of various concentrations of water (Figure 2). Increased concentration of water correlates with increased current close to the second oxidation event, which is assigned to a catalytic process.

The catalytic wave observed upon addition of water suggests that compound **3** acts as water oxidation catalyst. In order to quantify the reaction products upon electrochemical oxidation, we performed controlled potential electrolysis (CPE) experiments at 0.57 V (vs Fc/Fc^+). Complex **3** was dissolved in a mixture of $MeCN/H_2O$ (19:1 v/v) with 0.1 M [*n*-Bu_4N][ClO_4] as supporting electrolyte. The experiments were performed in a two-compartment cell

separated by an anion-exchange membrane. In a typical experiment, with a total amount of 5.8 C passed charge over the course of 1.5 h (Figure S9), H_2O_2 was detected with a Faradaic efficiency of ~15% using a chemiluminescence method with 10-acetyl-3,7-dihydroxyphenoxazine in combination of horseradish peroxidase (Figure S1).[15] Addition of catalase to the reaction mixture after electrolysis produced O_2 as detected by gas chromatography, which is also consistent with the generation of H_2O_2 by **3** (Figure S2). The exact overpotential of the system remains undetermined due to the use of a mixture of solvents. The potential for water oxidation to O_2 drifts ~ 200 mV more positive in acetonitrile,[16] for example.

The low observed Faradaic yield for H_2O_2 formation could be due to side reactions between the highly reactive species generated upon oxidation, such as Mn-oxo or Mn-(hydro)peroxo species, with organic moieties. To test this hypothesis, CPE was conducted in the presence of 9,10-dihydroanthracene (0.1 M) as a source of weak C-H bond to react with the intermediates. H_2O_2 was not detected in this experiment and the combined Faradaic efficiency corresponding to 9,10-dihydroanthracene oxidation to anthracene and anthraquinone was 51% (Figure S10). CV control experiments show that there is no oxidative wave for 9,10-dihydroanthracene in the absence of **3** at the applied potential of CPE experiments (Figure S11). Stirring 9,10-dihydroanthracene in the presence of **3** without applied potential also results in no oxidized products. These observations are consistent with the generation of reactive intermediates that perform H-atom abstraction and oxygenation reactions of C-H bonds competitive with water oxidation. The lack of H_2O_2 formation and the significant increase of the Faradaic yield in the presence of 9,10-dihydroanthracene indicate a faster reaction between the intermediates and the weak C-H bonds of this substrate than both H_2O_2 formation and side reactions with the organic solvent.

To evaluate the stability of **3** during catalysis in more detail, electrochemical experiments reveal that the voltammogram traces remain unchanged for 200 continuous cycles over the course of 3 h (Figure S12). After these scans, rinsing the electrode gently without polishing gave no catalytic wave and no redox features in a fresh electrolyte solution (Figure S12). Similar rinsing experiments were performed after CPE and showed no consumption of charge (Figure S9). These observations suggest that there is no deposition of catalytically active metal species on the electrode. Furthermore, to test the possibility of formation of heterogeneous MnO_x catalysts via free Mn ions, chelating ligands were added to solutions of **3** during CV measurements. No decrease of catalytic current was observed (Figures S14–16).[17] Additionally, dynamic light scattering measurements do not detect any nanoparticles (Figure S20). These observations are consistent with the absence of MnO_x formation from **3** in our electrochemical experiments. To evaluate whether other clusters that may form under the reaction conditions for the synthesis of **3** in small concentrations could be the active catalysts, several preparations were tested leaving some of the reagents out (Figures S18–19). In all cases tested, smaller catalytic current was observed compared to **3** at the same concentration. Thus, the control experiments are consistent with **3** as the active molecular catalyst for water oxidation to H_2O_2.

In summary, we report the synthesis of tetranuclear manganese complexes displaying hydrogen bonding networks as more accurate structural models of the biological water

oxidation catalyst that include second coordination sphere interactions. In particular, a cluster displaying a terminal hydroxide ligand is reminiscent of structural motifs involving the dangler Mn center of the OEC. Hydrogen bond donors and acceptors stabilize the terminal hydroxide ligand. This species supports electrocatalytic water oxidation to H_2O_2, albeit in low yield, in a rare demonstration of function (O-O bond formation) with a structural model of the OEC. Related to the mechanism of the biological system, the present results suggest that a terminal Mn-hydroxide moiety can serve as precursor to O-O bond formation chemistry. Importantly, control experiments are inconsistent with the generation of a heterogeneous active species, and support complex **3** as a discrete and well-defined electrocatalyst for water oxidation. Complex **3** is also able to perform both H-atom abstraction and oxygenation reactions with 9,10-dihydroanthracene under electrocatalytic conditions. Current studies are focused on the mechanistic aspects of these transformations.

Supplementary Material

Refer to Web version on PubMed Central for supplementary material.

Acknowledgments

This research was supported by the NIH (R01-GM102687A). We thank L. M. Henling for assistance with crystallography, J.C. Tran for assistance with the characterization of the 4-*t*BuC$_6$H$_4$NHPzH, and B. M. Hunter for helpful discussion on H_2O_2 detection.

References

1. (a) Lewis NS, Nocera DG. Proc. Natl. Acad. Sci. U.S.A. 2006; 103:15729–15735. [PubMed: 17043226] (b) Gray HB. Nat. Chem. 2009; 1:7–7. [PubMed: 21378780]
2. (a) Yano J, Yachandra V. Chem. Rev. 2014; 114:4175–4205. [PubMed: 24684576] (b) Blakemore JD, Crabtree RH, Brudvig GW. Chem. Rev. 2015; 115:12974–13005. [PubMed: 26151088] (c) Vinyard DJ, Ananyev GM, Dismukes GC. Annu. Rev. Biochem. 2013; 82:577–606. [PubMed: 23527694] (d) Kärkäs MD, Åkermark B. Dalton Trans. 2016; 45:14421–14461. [PubMed: 27142095]
3. (a) Ferreira KN, Iverson TM, Maghlaoui K, Barber J, Iwata S. Science. 2004; 303:1831–1838. [PubMed: 14764885] (b) Umena Y, Kawakami K, Shen JR, Kamiya N. Nature. 2011; 473:55–65. [PubMed: 21499260] (c) Suga M, Akita F, Hirata K, Ueno G, Murakami H, Nakajima Y, Shimizu T, Yamashita K, Yamamoto M, Ago H, Shen JR. Nature. 2015; 517:99–103. [PubMed: 25470056] (d) Young ID, Ibrahim M, Chatterjee R, Gul S, Fuller FD, Koroidov S, Brewster AS, Tran R, Alonso-Mori R, Kroll T, et al. Nature. 2016; 540:453–457. [PubMed: 27871088]
4. Cox N, Retegan M, Neese F, Pantazis DA, Boussac A, Lubitz W. Science. 2014; 345:804–808. [PubMed: 25124437]
5. Tsui EY, Kanady JS, Agapie T. Inorg. Chem. 2013; 52:13833–13848. [PubMed: 24328344]
6. (a) Zhang CX, Chen CH, Dong HX, Shen JR, Dau H, Zhao JQ. Science. 2015; 348:690–693. [PubMed: 25954008] (b) Kanady JS, Lin PH, Carsch KM, Nielsen RJ, Takase MK, Goddard WA, Agapie T. J. Am. Chem. Soc. 2014; 136:14373–14376. [PubMed: 25241826] (c) Mukherjee S, Stull JA, Yano J, Stamatatos TC, Pringouri K, Stich TA, Abboud KA, Britt RD, Yachandra VK, Christou G. Proc. Natl. Acad. Sci. U.S.A. 2012; 109:2257–2262. [PubMed: 22308383] (d) Kanady JS, Tsui EY, Day MW, Agapie T. Science. 2011; 333:733–736. [PubMed: 21817047]
7. (a) Limburg J, Vrettos JS, Liable-Sands LM, Rheingold AL, Crabtree RH, Brudvig GW. Science. 1999; 283:1524–1527. [PubMed: 10066173] (b) Naruta Y, Sasayama M, Sasaki T. Angew. Chem. Int. Ed. 1994; 33:1839–1841.(c) Karlsson EA, Lee BL, Åkermark T, Johnston EV, Kärkäs MD, Sun JL, Hansson O, Bäckvall J, Åkermark B. Angew. Chem. Int. Ed. 2011; 50:11715–11718.(d) Najafpour MM, Renger G, Holynska M, Moghaddam AN, Aro EM, Carpentier R, Nishihara H,

Eaton-Rye JJ, Shen JR, Allakhverdiev SI. Chem. Rev. 2016; 116:2886–2936. [PubMed: 26812090] (e) Poulsen AK, Rompel A, McKenzie CJ. Angew. Chem. Int. Ed. 2005; 44:6916–6920.(f) Beckmann K, Uchtenhagen H, Berggren G, Anderlund MF, Thapper A, Messinger J, Styring S, Kurz P. Energ. Environ. Sci. 2008; 1:668–676.(g) Ruettinger W, Yagi M, Wolf K, Bernasek S, Dismukes GC. J. Am. Chem. Soc. 2000; 122:10353–10357.(h) Brimblecombe R, Kolling DRJ, Bond AM, Dismukes GC, Swiegers GF, Spiccia L. Inorg. Chem. 2009; 48:7269–7279. [PubMed: 19572724] (i) Dismukes GC, Brimblecombe R, Felton GAN, Pryadun RS, Sheats JE, Spiccia L, Swiegers GF. Acc. Chem. Res. 2009; 42:1935–1943. [PubMed: 19908827]

8. (a) Evangelisti F, More R, Hodel F, Luber S, Patzke GR. J. Am. Chem. Soc. 2015; 137:11076–11084. [PubMed: 26266575] (b) Yin QS, Tan JM, Besson C, Geletii YV, Musaev DG, Kuznetsov AE, Luo Z, Hardcastle KI, Hill CL. Science. 2010; 328:342–345. [PubMed: 20223949] (c) Stracke JJ, Finke RG. J. Am. Chem. Soc. 2011; 133:14872–14875. [PubMed: 21894961] (d) Brimblecombe R, Swiegers GF, Dismukes GC, Spiccia L. Angew. Chem. Int. Ed. 2008; 47:7335–7338.(e) Hocking RK, Brimblecombe R, Chang LY, Singh A, Cheah MH, Glover C, Casey WH, Spiccia L. Nat. Chem. 2011; 3:461–466. [PubMed: 21602861] (f) McCool NS, Robinson DM, Sheats JE, Dismukes GC. J. Am. Chem. Soc. 2011; 133:11446–11449. [PubMed: 21739983] (g) Berardi S, La Ganga G, Natali M, Bazzan I, Puntoriero F, Sartorel A, Scandola F, Campagna S, Bonchio M. J. Am. Chem. Soc. 2012; 134:11104–11107. [PubMed: 22716164] (h) Smith PF, Kaplan C, Sheats JE, Robinson DM, McCool NS, Mezle N, Dismukes GC. Inorg. Chem. 2014; 53:2113–2121. [PubMed: 24498959] (i) Ullman AM, Liu Y, Huynh M, Bediako DK, Wang HS, Anderson BL, Powers DC, Breen JJ, Abruna HD, Nocera DG. J. Am. Chem. Soc. 2014; 136:17681–17688. [PubMed: 25407218] (j) Nguyen AI, Ziegler MS, Ona-Burgos P, Sturzbecher-Hohne M, Kim W, Bellone DE, Tilley TD. J. Am. Chem. Soc. 2015; 137:12865–12872. [PubMed: 26390993] (k) Smith PF, Hunt L, Laursen AB, Sagar V, Kaushik S, Calvinho KUD, Marotta G, Mosconi E, De Angelis F, Dismukes GC. J. Am. Chem. Soc. 2015; 137:15460–15468. [PubMed: 26593692] (l) Okamura M, Kondo M, Kuga R, Kurashige Y, Yanai T, Hayami S, Praneeth VKK, Yoshida M, Yoneda K, Kawata S, Masaoka S. Nature. 2016; 530:465–468. [PubMed: 26863188] (m) Cady CW, Crabtree RH, Brudvig GW. Coord. Chem. Rev. 2008; 252:444–455. [PubMed: 21037800]

9. Weinberg DR, Gagliardi CJ, Hull JF, Murphy CF, Kent CA, Westlake BC, Paul A, Ess DH, McCafferty DG, Meyer TJ. Chem. Rev. 2012; 112:4016–4093. [PubMed: 22702235]

10. (a) Shirin Z, Hammes BS, Young VG, Borovik AS. J. Am. Chem. Soc. 2000; 122:1836–1837.(b) MacBeth CE, Gupta R, Mitchell-Koch KR, Young VG, Lushington GH, Thompson WH, Hendrich MP, Borovik AS. J. Am. Chem. Soc. 2004; 126:2556–2567. [PubMed: 14982465] (c) Shook RL, Peterson SM, Greaves J, Moore C, Rheingold AL, Borovik AS. J. Am. Chem. Soc. 2011; 133:5810–5817. [PubMed: 21425844] (d) Borovik AS. Acc. Chem. Res. 2005; 38:54–61. [PubMed: 15654737] (e) Ford CL, Park YJ, Matson EM, Gordon Z, Fout AR. Science. 2016; 354:741–743. [PubMed: 27846604] (f) Zong R, Thummel RP. J. Am. Chem. Soc. 2005; 127:12802–12803. [PubMed: 16159265] (g) Dogutan DK, McGuire R, Nocera DG. J. Am. Chem. Soc. 2011; 133:9178–9180. [PubMed: 21604700] (h) Chang CJ, Chng LL, Nocera DG. J. Am. Chem. Soc. 2003; 125:1866–1876. [PubMed: 12580614] (i) Carver CT, Matson BD, Mayer JM. J. Am. Chem. Soc. 2012; 134:5444–5447. [PubMed: 22394189] (j) Rigsby ML, Wasylenko DJ, Pegis ML, Mayer JM. J. Am. Chem. Soc. 2015; 137:4296–4299. [PubMed: 25798713]

11. A CSD search of small Mn clusters displaying terminal hydroxide ligands resulted in few examples characterized by crystallography: Wieghardt K, Bossek U, Nuber B, Weiss J, Bonvoisin J, Corbella M, Vitols SE, Girerd JJ. J. Am. Chem. Soc. 1988; 110:7398–7411.Pal S, Armstrong WH. Inorg. Chem. 1992; 31:5417–5423.Pal S, Chan MK, Armstrong WH. J. Am. Chem. Soc. 1992; 114:6398–6406.Chen HY, Collomb MN, Duboc C, Blondin G, Riviere E, Faller JW, Crabtree RH, Brudvig GW. Inorg. Chem. 2005; 44:9567–9573. [PubMed: 16323946] Corbella M, Costa R, Ribas J, Fries PH, Latour JM, Ohrstrom L, Solans X, Rodriguez V. Inorg. Chem. 1996; 35:1857–1865.Ng GKY, Ziller JW, Borovik AS. Chem. Commun. 2012; 48:2546–2548.

12. Tsui EY, Kanady JS, Day MW, Agapie T. Chem. Commun. 2011; 47:4189–4191.

13. (a) de Ruiter G, Thompson NB, Lionetti D, Agapie T. J. Am. Chem. Soc. 2015; 137:14094–14106. [PubMed: 26390375] (b) de Ruiter G, Thompson NB, Takase MK, Agapie T. J. Am. Chem. Soc. 2016; 138:1486–1489. [PubMed: 26760217] (c) de Ruiter G, Carsch KM, Gul S, Chatterjee R, Thompson NB, Takase MK, Yano J, Agapie T. Angew. Chem. Int. Ed. 2017; 56:4772–4776.(d)

Kanady JS, Tran R, Stull JA, Lu L, Stich TA, Day MW, Yano J, Britt RD, Agapie T. Chem. Sci. 2013; 4:3986–3996. [PubMed: 24163730]

14. Sickerman NS, Park YJ, Ng GKY, Bates JE, Hilkert M, Ziller JW, Furche F, Borovik AS. Dalton Trans. 2012; 41:4358–4364. [PubMed: 22334366]
15. Zhou MJ, Diwu ZJ, PanchukVoloshina N, Haugland RP. Anal. Biochem. 1997; 253:162–168. [PubMed: 9367498]
16. Pegis ML, Roberts JAS, Wasylenko DJ, Mader EA, Appel AM, Mayer JM. Inorg. Chem. 2015; 54:11883–11888. [PubMed: 26640971]
17. A MnO_x catalyst has been shown to produce H_2O_2 only at basic pH: Izgorodin A, Izgorodina E, MacFarlane DR. Energ. Environ. Sci. 2012; 5:9496–9501.

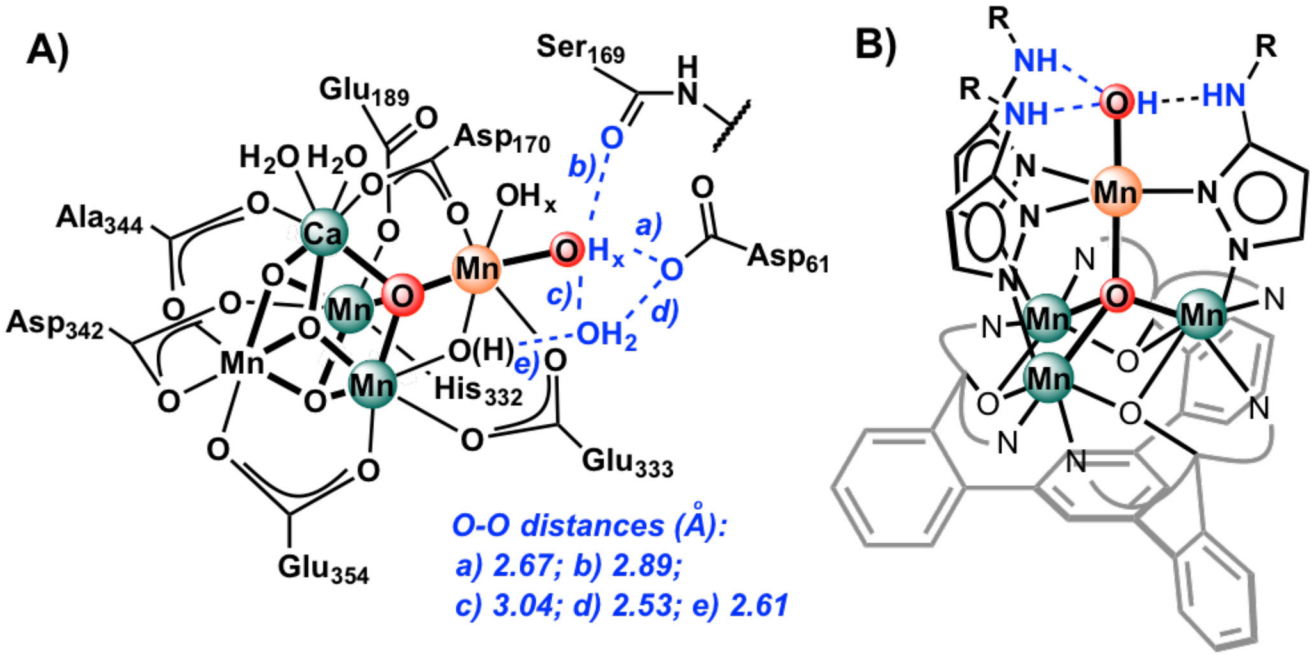

Figure 1.

A) Drawing of the OEC (PDB 4UB8) highlighting a tetranuclear cluster including the dangling Mn (orange) and H-bonding network (blue)[3b,d]; **B**) Target synthetic model.

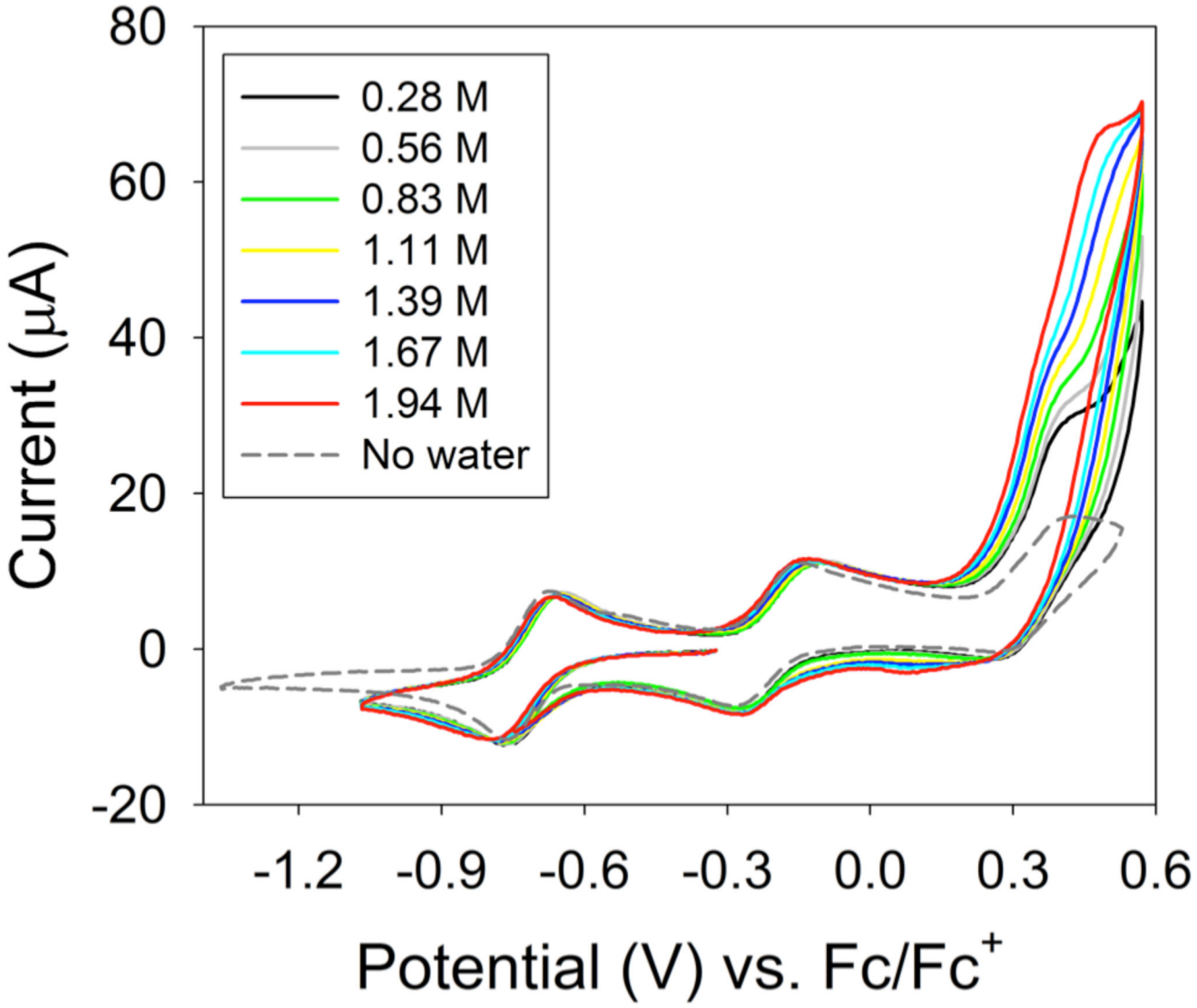

Figure 2.

Cyclic voltammograms of 1.0 mM of [LMn_3(4-*t*$BuC_6H_4NHPz)_3OMn(OH)$][OTf] (**3**) in MeCN without water (gray dash) and in the presence of water with increasing concentration (other colors). Conditions: 0.1 M [*n*-Bu_4N][ClO_4], GC working electrode, 0.07 cm^2, Pt wire counter electrode, scan rate: 100 mV/s.

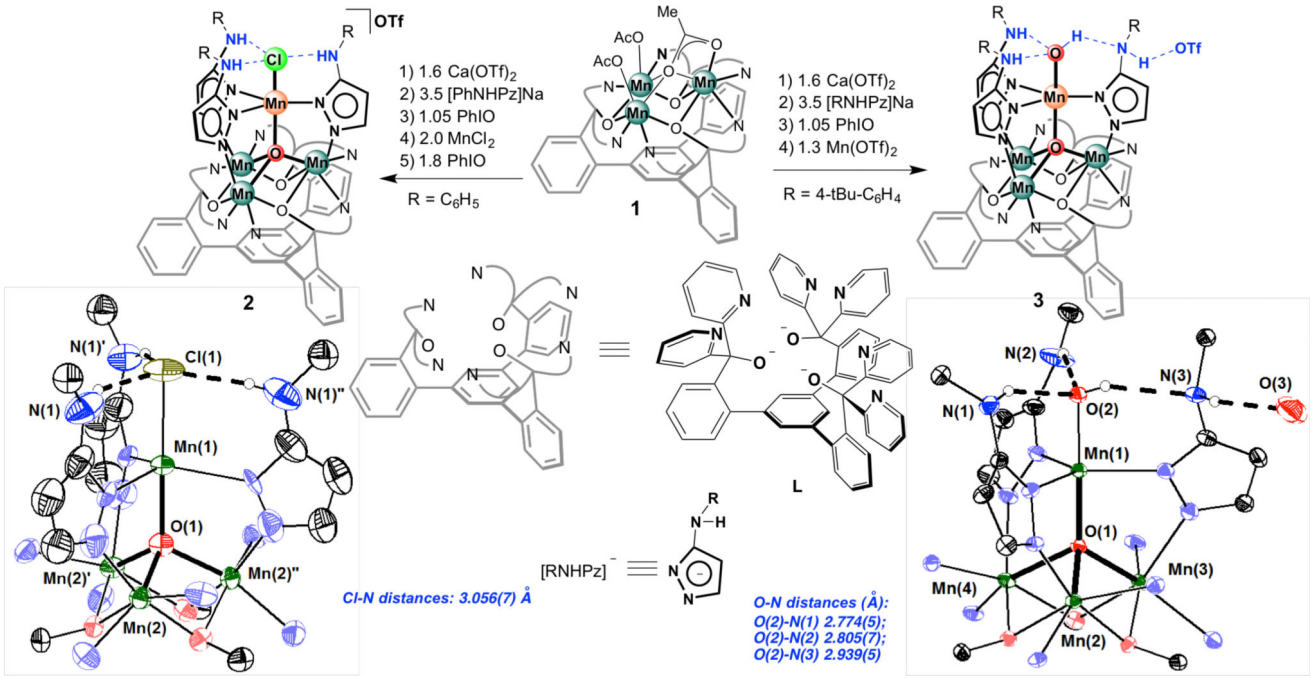

Scheme 1.

Synthesis of tetranuclear manganese complexes and crystal structures of **2** and **3**. Thermal ellipsoids are shown at the 50% probability level. Parts of the ligands, hydrogen atoms, triflate, and co-crystallized solvent molecules are not shown for clarity.